

This article was downloaded by:

On: 23 January 2011

Access details: *Access Details: Free Access*

Publisher *Taylor & Francis*

Informa Ltd Registered in England and Wales Registered Number: 1072954 Registered office: Mortimer House, 37-41 Mortimer Street, London W1T 3JH, UK



Journal of Coordination Chemistry

Publication details, including instructions for authors and subscription information:

<http://www.informaworld.com/smpp/title~content=t713455674>

Synthesis and structural characterization of ferrocenyl indenyl derivatives

Mei-Hua Luo^{ab}; Li-Min Han^a; Ning Zhu^a; Hai-Long Hong^a; Rui-Jun Xie^a; Quan-Ling Suo^a; Lin-Hong Weng^c

^a Chemical Engineering College, Inner Mongolia University of Technology, Hohhot 010051, P.R. China

^b Chemistry and Chemical Engineering School, Inner Mongolia University, Hohhot 010021, P.R. China

^c Department of Chemistry, Fudan University, Shanghai 200433, P.R. China

Online publication date: 13 October 2010

To cite this Article Luo, Mei-Hua , Han, Li-Min , Zhu, Ning , Hong, Hai-Long , Xie, Rui-Jun , Suo, Quan-Ling and Weng, Lin-Hong(2010) 'Synthesis and structural characterization of ferrocenyl indenyl derivatives', *Journal of Coordination Chemistry*, 63: 21, 3805 – 3815

To link to this Article: DOI: 10.1080/00958972.2010.521937

URL: <http://dx.doi.org/10.1080/00958972.2010.521937>

PLEASE SCROLL DOWN FOR ARTICLE

Full terms and conditions of use: <http://www.informaworld.com/terms-and-conditions-of-access.pdf>

This article may be used for research, teaching and private study purposes. Any substantial or systematic reproduction, re-distribution, re-selling, loan or sub-licensing, systematic supply or distribution in any form to anyone is expressly forbidden.

The publisher does not give any warranty express or implied or make any representation that the contents will be complete or accurate or up to date. The accuracy of any instructions, formulae and drug doses should be independently verified with primary sources. The publisher shall not be liable for any loss, actions, claims, proceedings, demand or costs or damages whatsoever or howsoever caused arising directly or indirectly in connection with or arising out of the use of this material.

Synthesis and structural characterization of ferrocenyl indenyl derivatives

MEI-HUA LUO^{†‡}, LI-MIN HAN^{*†}, NING ZHU[†], HAI-LONG HONG[†],
RUI-JUN XIE[†], QUAN-LING SUO[†] and LIN-HONG WENG[§]

[†]Chemical Engineering College, Inner Mongolia University of Technology,
Hohhot 010051, P.R. China

[‡]Chemistry and Chemical Engineering School, Inner Mongolia University,
Hohhot 010021, P.R. China

[§]Department of Chemistry, Fudan University, Shanghai 200433, P.R. China

(Received 25 June 2010; in final form 2 August 2010)

In this study, four ferrocenyl indenyl derivatives, $C_9H_7-C\equiv C-Fc$ (**1**), $C_9H_7-C\equiv C-Ph-Fc$ (**2**), $C_9H_7-C\equiv C-Ph-C\equiv C-Fc$ (**3**), and $C_9H_7-Ph-C\equiv C-Fc$ (**4**) (where C_9H_7 =indenyl; $Fc=C_5H_5FeC_5H_4$; $Ph=C_6H_5$), have been synthesized by Sonogashira and Suzuki cross-coupling reactions and characterized by elemental analysis, and FT-IR, 1H , ^{13}C -NMR, and MS spectroscopic methods, respectively. The molecular structures of **1**, **2**, and **4** were determined by X-ray single crystal diffraction. Two molecules appeared in the crystal structure of **4**, and they interact through an intermolecular hydrogen bond. The electrochemical redox potential differences in **1–4** were investigated using cyclic voltammetry and calculations.

Keywords: Indenyl; Ferrocenyl; Cross-coupling; Molecular structure

1. Introduction

Indenyl derivatives and their coordination compounds have received attention due to the special coordinated behavior and favorable catalytic and electrochemical activities of indenyl metal complexes [1–7]. For example, electronic communication of metallic centers in indenyl bimetallic complexes and the catalytic activities of indenyl cobalt complexes had been validated by Lee and Ceccon [8, 9]. Ferrocenyl indenyl derivatives have evoked increased interest, are more facily prepared, and serve as a redox switch to modulate activities of other metallic centers. For instance, Santi has reported the synthesis and mixed valence properties in ferrocenyl-based bimetallic complexes [10–13]. Wang has reported the synthesis and crystal structure of ferrocene-bridged indenyl carbonyl complexes of iron, ruthenium and molybdenum [14]. Gaede [15] has reported crystal structures of ferrocene-substituted indenyl complexes [16–22].

*Corresponding author. Email: hanlimin_442@hotmail.com

We find that synthesis of ferrocenyl indenyl ligands is the key factor for further construction of ferrocene-substituted indenyl complexes [16–22]. Hence, preparation of new ferrocenyl indenyl ligands is helpful for construction of their metal complexes and investigating the interactions of metallic centers.

In this article, four ferrocenyl indenyl derivatives, $C_9H_7-C\equiv C-Fc$ (**1**), $C_9H_7-C\equiv C-C_6H_5-Fc$ (**2**), $C_9H_7-C\equiv C-C_6H_5-C\equiv C-Fc$ (**3**), and $C_9H_7-C_6H_5-C\equiv C-Fc$ (**4**), were synthesized by Sonogashira and Suzuki cross-coupling reactions, and the molecular and crystal structures of **1**, **2**, and **4** were determined by X-ray single crystal diffraction analysis. In these molecules, the ferrocenyl and indenyl parts were assembled into a partially conjugated system *via* the phenyl and ethynyl groups, providing ligands for the further design of functional complexes.

2. Experimental

2.1. General procedures

All reactions and manipulations were carried out using standard Schlenk techniques under an atmosphere of argon. All reactions were monitored with thin-layer chromatography (TLC). Solvents were purified, dried, and distilled under argon prior to use. Column chromatographic separations and purifications were performed on 200–300 mesh silica gel or neutral alumina. Here, 4-Bromo-phenyl-ethynylferrocene [23], 4-ethynyl-phenylferrocene [24], ethynylferrocene [25], 4-iodo-phenyl-ethynylferrocene [26], and 2-ethynyl-indene [27] were prepared by literature methods.

IR spectra were recorded on a Nicolet FT-IR spectrometer. Elemental analyses were carried out on an Elementar var III-type analyzer. 1H - and ^{13}C -NMR spectra in $CDCl_3$ were recorded on a Bruker Avance-500 MHz spectrometer. Mass spectra were determined using Polaris Q MS, Micromass LCT, and Agilent LC/MSD TOF instruments.

2.2. Synthesis of 2-indenyl-ethynylferrocene $C_9H_7-C\equiv C-Fc$ (**1**)

$Fc-C\equiv CH$ (1.06 g, 5.0 mmol), 2-bromo-indene (1.08 g, 5.5 mmol), $Pd(PPh_3)_2Cl_2$ (105 mg, 0.15 mmol), and CuI (38 mg, 0.20 mmol) were dissolved in a mixture of THF (12 mL) and triethylamine (3 mL) and stirred for 6 h at $40^\circ C$. Then, solvent was removed under reduced pressure and the residue purified by column chromatography. An orange band was afforded using hexane/benzene (4:1, v/v) as eluant. Single crystal of **1** was obtained by recrystallizing **1** from hexane/dichloromethane (4:1, v/v) at room temperature. Yield: 84%; m.p. 147 – $148^\circ C$. Anal. Calcd for $C_{21}H_{16}Fe$: C, 77.80 and H, 4.97. Found: C, 77.81 and H, 4.97%. IR (KBr disc, cm^{-1}): ν 3100w, 3060w, 3011w, 2918w, 2195m, 1634m, 1606w, 1103w, 1028s, 869m, 833m, and 754s. 1H -NMR ($DCCl_3$, δ): 7.20–7.42 (m, 4 H, indenyl, C_6H_4), 7.07 (s, 1 H, indenyl, CH), 3.58 (s, 2 H, indenyl, CH_2); and 4.26, 4.51 (s, 9 H, $C_5H_5FeC_5H_4$). Also, ^{13}C -NMR ($CDCl_3$, δ): 144.41, 142.75, 136.01, 128.01, 126.71, 125.37, 123.46, 121.09, 42.86 (indenyl); 93.31, 83.05 ($C\equiv C$); 71.40, 70.08, 69.01, and 65.46 (Fc). HRMS(ESI, m/z): 324.0637 (M^+).

2.3. Synthesis of 4-(2-indenylethynyl)phenylferrocene $C_9H_7-C\equiv C-C_6H_4-Fc$ (**2**)

Fc- $C_6H_4-C\equiv CH$ (572 mg, 2.0 mmol), 2-bromo-indene (437 mg, 2.2 mmol), Pd(PPh₃)₂Cl₂ (42 mg, 0.06 mmol), and CuI (15 mg, 0.08 mmol) were dissolved in THF (10 mL) and triethylamine (2 mL), and stirred for 14 h at room temperature. The solvent was removed from the filtrate under reduced pressure and the residue purified by neutral alumina column chromatography. A yellow band was afforded by using hexane/dichloromethane (5:1, v/v) as eluant. Single crystals of **2** were obtained by recrystallizing **2** from hexane/dichloromethane (4:1, v/v) at room temperature. Yield: 54%; m.p. 223–224°C. Anal. Calcd for C₂₇H₂₀Fe: C, 81.01; and H, 5.04. Found: C, 80.59; H, 4.92%. IR (KBr disc, cm⁻¹): ν 3089 m, 3061 m, 3041 m, 2917 m, 2891 w, 2187 w, 1600 m, 1518 s, 1104 s, 1002 m, 818 s, and 753 s. ¹H-NMR (DCCl₃, δ): 7.23–7.46 (m, 8H, phenyl, C₆H₄; indenyl, 4CH), 7.16 (s, 1H, indenyl, CH), and 3.64 (s, 2H, indenyl, CH₂); 4.07, 4.38, and 4.70 (s, 9H, C₅H₅FeC₅H₄); ¹³C-NMR (CDCl₃, δ): 144.26, 142.98, 139.92, 136.98, 131.50, 127.51, 126.77, 125.84, 125.63, 123.56, 121.32, 120.41, 94.53, and 42.75 (phenyl, indenyl); 86.79, 84.42(C \equiv C); 69.85, 69.51, and 66.58(Fc). HRMS (ESI, m/z): 400.0901 (M⁺).

2.4. Synthesis of 4-(2-indenylethynyl)-phenyl-ethynylferrocene $C_9H_7-C\equiv C-C_6H_4-C\equiv C-Fc$ (**3**)

Fc- $C\equiv C-C_6H_4-I$ (411 mg, 1.0 mmol), 2-ethynylindene (214 mg, 1.5 mmol), Pd(PPh₃)₂Cl₂ (23 mg, 0.03 mmol), and CuI (8 mg, 0.04 mmol) were dissolved in THF (10 mL) and triethylamine (5 mL), and stirred for 16 h at 18°C. The solvent was removed from the filtrate under reduced pressure and the residue purified by neutral alumina column chromatography. An orange band was afforded using hexane/benzene (1:1, v/v) as eluent. Orange crystals of **3** were obtained by recrystallizing **3** from hexane/dichloromethane (4:1, v/v) at room temperature. Yield: 42%; m.p. 300°C (dec.). Anal. Calcd for C₂₉H₂₀Fe: C, 82.09 and H, 4.75. Found: C, 81.18; H, 4.70%. IR (KBr disc, cm⁻¹): ν 3093 w, 3057 m, 3042 m, 2909 w, 2205 s, 2197 s, 1603 m, 1509 s, 1105 m, 1002 m, 825 vs, and 754 m. ¹H-NMR (DCCl₃, δ): 7.26–7.45 (m, 8H, phenyl C₆H₄; indenyl, 4CH), 7.17 (s, 1H, indenyl, CH), 3.63 (s, 2H, indenyl, CH₂); 4.30, and 4.56 (s, 9H, C₅H₅FeC₅H₄). ¹³C-NMR (CDCl₃, δ): 144.11, 143.03, 137.60, 136.45, 131.33, 127.11, 126.81, 125.82, 123.76, 123.59, 122.42, 121.46, 94.00, 90.67, and 42.7 (phenyl, indenyl); 88.36, 85.61 (C \equiv C); 71.71, 70.41, 69.38, and 65.49 (Fc). MS (EI, m/z) 424 (M⁺).

2.5. Synthesis of 4-(2-indenyl)-phenyl-ethynylferrocene $C_9H_7-C_6H_4-C\equiv C-Fc$ (**4**)

n-Butyllithium (2.85 mol L⁻¹ in hexane, 0.96 mL, 2.75 mmol) and 4-bromo-phenylethynylferrocene Fc- $C\equiv C-C_6H_4-Br$ (911 mg, 2.5 mmol) were added into THF (15 mL) at -78°C. The solution was stirred for 1 h at -78°C; then B(O-*i*-Pr)₃ (0.9 mL, 3.9 mmol) was added. The resulting solution was allowed to warm from -78°C to room temperature and stirred overnight. Toluene (15 mL), ethanol (15 mL), water (6 mL), Na₂CO₃ (398 mg, 3.75 mmol), 2-bromo-indene (685 mg, 3.5 mmol), and Pd(PPh₃)₄ (87 mg, 0.075 mmol) were added to the solution and refluxed for 24 h. The resulting solution was extracted by dichloromethane and the organic phase combined, dried

using anhydrous MgSO_4 , filtered, and solvent removed under reduced pressure. The residue was purified by silica gel column chromatography giving an orange-red band, using hexane/dichloromethane (5:1, v/v) as eluant. Orange-red crystals of **4** were obtained by recrystallizing from hexane/dichloromethane (4:1, v/v) at room temperature. Yield: 42%; m.p. 213–214°C. Anal. Calcd for $\text{C}_{27}\text{H}_{20}\text{Fe}$: C, 81.01 and H, 5.04. Found: C, 80.84 and H, 4.89%. IR (KBr disc, cm^{-1}): ν 3076 m, 3022w, 2897w, 2205 s, 1603w, 1508vs, 1104 s, 1001 m, 822vs, and 749 s. $^1\text{H-NMR}$ (DCCl_3 , δ): 7.21–7.59 (m, 8H, phenyl C_6H_4 ; indenyl, 4CH), 3.80 (s, 2H, indenyl, CH); 4.31 and 4.58 (s, 9H, $\text{C}_5\text{H}_5\text{FeC}_5\text{H}_4$); $^{13}\text{C-NMR}$ (CDCl_3 , δ): 145.73, 145.22, 143.17, 135.19, 131.67, 127.22, 126.69, 125.42, 124.97, 123.68, 122.82, 121.11, and 38.89 (phenyl, indenyl); 89.41, 85.95 ($\text{C}\equiv\text{C}$); 71.64, 70.37, 69.26, and 65.85 (Fc, indenyl). HRMS(ESI, m/z): 400.0905 (M^+).

2.6. X-ray crystallography of **1**, **2**, and **4**

Crystals of **1**, **2**, and **4** were mounted on glass fibers. All measurements were made on a Bruker SMART APEX CCD diffractometer with graphite monochromated $\text{Mo-K}\alpha$ ($\lambda = 0.71073 \text{ \AA}$) radiation. All data were collected at 20°C using φ and ω scan techniques. All structures were solved by direct methods and expanded using Fourier techniques [28]. An absorption correction based on SADABS was applied [29]. All non-hydrogen atoms were refined by full matrix least-squares on F^2 . Hydrogens were located and refined by geometric method. The cell refinement, data collection, and reduction were performed by Bruker SMART and SAINT [30]. The structure solution and refinement were performed by SHELXSL97 [31]. Crystal data and details of measurements are shown in table 1.

2.7. Cyclic voltammetry of **1**, **2**, **3**, and **4**

The platinum disc (0.8 mm) was used as working electrode for cyclic voltammetry. The electrode surface was polished with 0.05 μm alumina before each run. The auxiliary electrode was a coiled platinum wire. The reference electrode was an $\text{Ag}|\text{Ag}^+$ electrode. The supporting electrolyte used in all electrochemical experiments was tetra-*n*-butylammonium hexafluorophosphate (TBAHFP, 0.5 mol L^{-1}). Samples of **1**, **2**, **3**, and **4** were dissolved in dichloromethane with concentration 1 mmol. The potentiostat was CHI-760C. We employed argon as purge gas to eliminated oxygen from the one-compartment cell before electrochemical runs.

3. Results and discussion

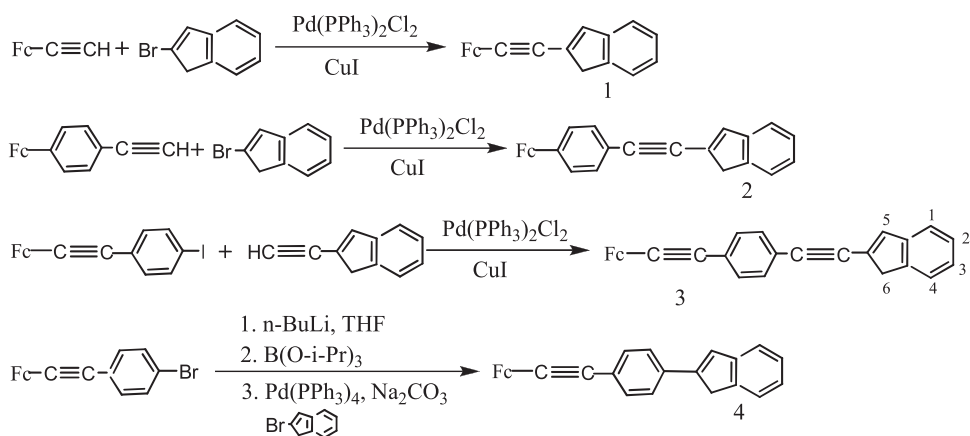
3.1. Synthesis and characterization of **1**, **2**, **3**, and **4**

The compounds, $\text{C}_9\text{H}_7\text{-C}\equiv\text{C-Fc}$ (**1**), $\text{C}_9\text{H}_7\text{-C}\equiv\text{C-C}_6\text{H}_5\text{-Fc}$ (**2**), and $\text{C}_9\text{H}_7\text{-C}\equiv\text{C-C}_6\text{H}_5\text{-C}\equiv\text{C-Fc}$ (**3**), were synthesized by Sonogashira cross-coupling of $\text{Fc-C}\equiv\text{CH}$, $\text{Fc-C}_6\text{H}_4\text{-C}\equiv\text{CH}$, and $\text{C}_9\text{H}_7\text{-C}\equiv\text{CH}$ with $\text{C}_9\text{H}_7\text{-Br}$ and $\text{Fc-C}\equiv\text{C-C}_6\text{H}_4\text{-I}$, respectively. $\text{C}_9\text{H}_7\text{-C}_6\text{H}_5\text{-C}\equiv\text{C-Fc}$ (**4**) was obtained by Suzuki cross-coupling of $\text{Fc-C}\equiv\text{C-C}_6\text{H}_4\text{-Br}$ with $\text{C}_9\text{H}_7\text{-Br}$. The reactions carried out in this study are illustrated in scheme 1.

Table 1. Crystallographic data and relevant structural parameters of **1**, **2**, and **4**.

Identification code	1	2	4
Empirical formula	C ₂₁ H ₁₆ Fe	C ₂₇ H ₂₀ Fe	C ₂₇ H ₂₀ Fe
Formula weight	324.19	400.28	400.28
Temperature (K)	293(2)	293(2)	293(2)
Wavelength (Å)	0.71073	0.71073	0.71073
Crystal system	Monoclinic	Monoclinic	Monoclinic
Space group	C2/c	P2(1)/c	P2(1)
Unit cell dimensions (Å, °)			
<i>a</i>	26.540(8)	19.313(4)	14.476(7)
<i>b</i>	9.714(3)	7.6810(18)	7.622(4)
<i>c</i>	11.726(4)	13.426(3)	17.763(8)
α	90.00	90.00	90.00
β	95.376(4)	103.661(5)	98.865(7)
γ	90.00	90.00	90.00
Volume (Å ³), <i>Z</i>	3010.0(16), 8	1935.2(8), 4	1936.5(16), 4
Density (calculated) (Mg m ⁻³)	1.431	1.374	1.370
Absorption coefficient (mm ⁻¹)	0.994	0.788	0.788
<i>F</i> (000)	1344	832	832
Crystal size (mm ³)	0.15 × 0.10 × 0.08	0.12 × 0.10 × 0.06	0.12 × 0.10 × 0.06
θ range for data collection (°)	2.79–26.01	1.09–26.01	1.42–25.99
Limiting indices	–32 ≤ <i>h</i> ≤ 30; –10 ≤ <i>k</i> ≤ 11; –14 ≤ <i>l</i> ≤ 14	–21 ≤ <i>h</i> ≤ 23; –9 ≤ <i>k</i> ≤ 9; –14 ≤ <i>l</i> ≤ 16	–15 ≤ <i>h</i> ≤ 17; –9 ≤ <i>k</i> ≤ 9; –20 ≤ <i>l</i> ≤ 21
Reflections collected	6687	8683	8947
Independent reflections	2931	3804	4080
Completeness to θ (%)	98.9	99.7	99.4
Maximum and minimum transmission	0.9247 and 0.8652	0.9542 and 0.9114	0.9543 and 0.9114
Data/restraints/parameters	2931/0/199	3804/0/253	4080/1/506
Goodness-of-fit on <i>F</i> ²	1.025	1.003	1.017
Final <i>R</i> indices [<i>I</i> > 2 σ (<i>I</i>)]	<i>R</i> ₁ = 0.0322, <i>wR</i> ₂ = 0.0828	<i>R</i> ₁ = 0.0469, <i>wR</i> ₂ = 0.1112	<i>R</i> ₁ = 0.0407, <i>wR</i> ₂ = 0.0975
<i>R</i> indices (all data)	<i>R</i> ₁ = 0.0389, <i>wR</i> ₂ = 0.0869	<i>R</i> ₁ = 0.0827, <i>wR</i> ₂ = 0.1385	<i>R</i> ₁ = 0.0539, <i>wR</i> ₂ = 0.1040
Largest difference peak and hole (e Å ⁻³)	0.347 and –0.316	0.316 and –0.225	0.509 and –0.212
Weighing scheme	Calcd <i>w</i> = 1/[$\sigma^2(F_o^2)$ + (0.0519 <i>P</i>) ² + 1.1022 <i>P</i>], <i>P</i> = (<i>F</i> _o ² + 2 <i>F</i> _c ²)/3	Calcd <i>w</i> = 1/[$\sigma^2(F_o^2)$ + (0.0672 <i>P</i>) ² + 0.0000 <i>P</i>], <i>P</i> = (<i>F</i> _o ² + 2 <i>F</i> _c ²)/3	Calcd <i>w</i> = 1/[$\sigma^2(F_o^2)$ + (0.0503 <i>P</i>) ² + 0.0000 <i>P</i>], <i>P</i> = (<i>F</i> _o ² + 2 <i>F</i> _c ²)/3

Compounds **1–4** contain ferrocenyl and indenyl fragments linked by conjugated ethynyl or phenylethynyl spacers. The air-stable compounds are yellow to red and soluble in non-polar solvents such as benzene and polar solvents such as THF or dichloromethane; **1–4** were confirmed by elemental analysis FT-IR, ¹H-NMR, ¹³C-NMR, and MS methods. The IR spectrum of **3** shows two strong –C≡C– stretching bands at 2205 and 2197 cm⁻¹, which identify two different –C≡C– units in **3**. Bands at 3093, 3057, and 3042 cm⁻¹ may be C–H stretching frequencies in the unsaturated phenyl, Fc, or indenyl. The absorption at 2909 cm⁻¹ is the asymmetric C–H stretching frequency, which indicates a saturated carbon in the molecule. Absorptions at 1603 and 1509 cm⁻¹ can be attributed to –C=C– stretching vibration. In the ¹H-NMR spectrum



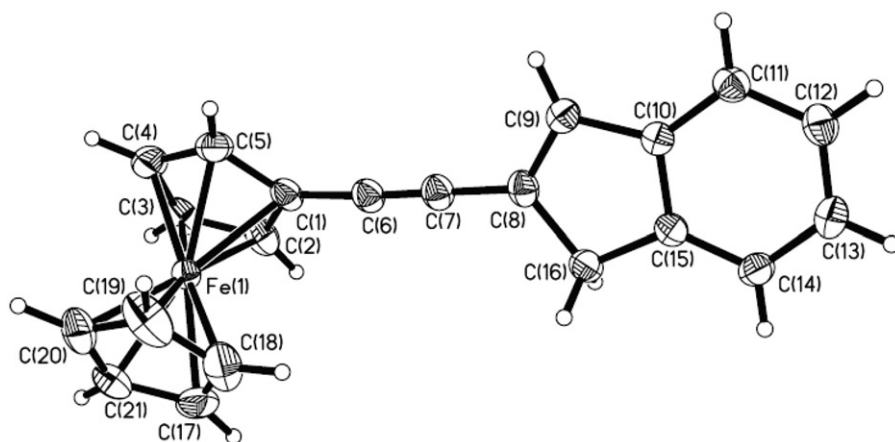
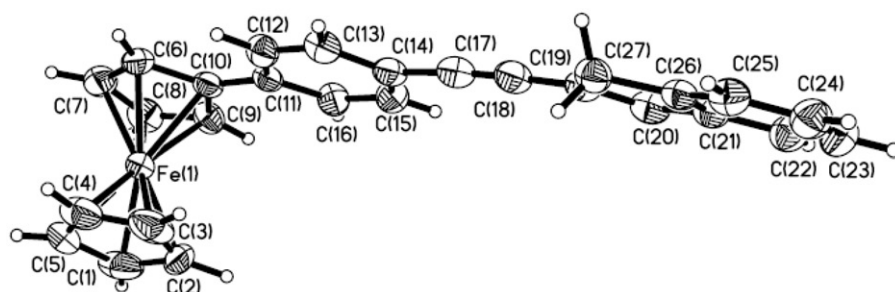
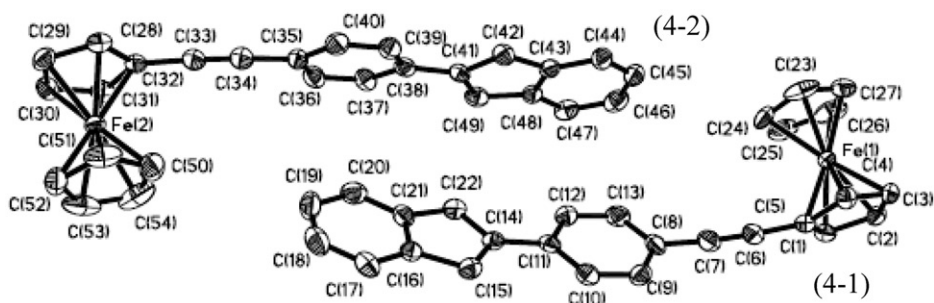
Scheme 1. The synthesis of 1-4.

of **3**, peaks between 7.26 and 7.45 ppm (8H) can be ascribed to four hydrogens of phenyl and four hydrogens at positions 1, 2, 3, and 4 of indenyl (see **3** in scheme 1). The peak at 7.17 ppm (1H) can be attributed to hydrogen at position 5 of indenyl. The peak at 3.63 ppm (2H) belongs to the hydrogens at position 6 of indenyl. The peaks between 4.30 and 4.56 ppm (9H) are attributed to nine hydrogens of ferrocenyl. In the $^{13}\text{C-NMR}$ spectrum of **3**, we ascribe 14 peaks between 144.11 and 90.67 ppm to 14 unsaturated carbons in phenyl and indenyl. The peak at 42.7 ppm belongs to carbon at position 6 of indenyl. Peaks between 88.36 and 85.61 ppm (4C) are carbons of $-\text{C}\equiv\text{C}-$ units. The carbons of ferrocenyl are at 71.71–65.49 ppm. The MS of **3** shows molecular ion at [424 (M^+)].

3.2. Molecular structures of 1, 2, and 4

The molecular structures of **1**, **2**, and **4** were determined by X-ray single crystal analysis. Crystal data and structural parameters are enumerated in table 1. The structures with atom numbering schemes are shown in figures 1, 2, and 3, and selected bond lengths and angles are listed in table 2.

Compound **1** contains ferrocenyl and indenyl groups linked by an ethynyl spacer (figure 1). The bond distances $\text{C}(6)\text{--}\text{C}(7)$ [1.197(3) Å] indicate a $-\text{C}\equiv\text{C}-$ triple bond. Bond distances of $\text{C}(1)\text{--}\text{C}(6)$ [1.426(3) Å] and $\text{C}(7)\text{--}\text{C}(8)$ [1.419(3) Å] are shorter than classical single bonds, suggesting electron delocalization. A shorter bond length of $\text{C}(8)\text{--}\text{C}(9)$ [1.364(3) Å], and two longer bond lengths $\text{C}(8)\text{--}\text{C}(16)$ [1.503(3) Å] and $\text{C}(15)\text{--}\text{C}(16)$ [1.496(3) Å] demonstrate conjugated double bond and non-conjugated single bonds in the five-membered ring of indenyl. The bond angles [$\text{C}(1)\text{--}\text{C}(6)\text{--}\text{C}(7)$, $176.4(2)^\circ$; $\text{C}(6)\text{--}\text{C}(7)\text{--}\text{C}(8)$, $179.5(2)^\circ$] prove that the carbon chain $\text{C}(1)\text{C}(6)\text{C}(7)\text{C}(8)$ is nearly linear. However, the dihedral angle of cyclopentadiene (Cp) plane of ferrocenyl to indenyl plane was 33.3° ; Cp and indenyl are not coplanar. This indicated ferrocenyl and indenyl were partially conjugated despite the fact that $\text{C}(1)\text{C}(6)\text{C}(7)\text{C}(8)$ is nearly linear and the bond lengths of $\text{C}(1)\text{--}\text{C}(6)$ and $\text{C}(7)\text{--}\text{C}(8)$ are shorter than the normal bond length of a single bond.

Figure 1. The molecular structure of **1**.Figure 2. The molecular structure of **2**.Figure 3. The molecular structure of **4** (the down molecule is 4-1, and the upper molecule is 4-2).

For **2**, C(17)–C(18) of 1.181(5) Å is shorter than that in **1** and exhibits $\text{C}\equiv\text{C}$ -character. Bond lengths of C(18)–C(19) and C(14)–C(17) are 1.416(6) and 1.438(6) Å, respectively, similar to that of **1**. C(19)–C(20), C(19)–C(27), C(20)–C(21), and C(26)–C(27) are 1.355(5), 1.480(5), 1.443(5), and 1.489(5) Å, respectively,

Table 2. Selected bond lengths (Å) and angles (°) for **1**, **2**, and **4**.

Bond lengths				Bond angles			
1							
C(1)–C(6)	1.426(3)	C(6)–C(7)	1.197(3)	C(1)–C(6)–C(7)	176.4(2)	C(6)–C(7)–C(8)	179.5(2)
C(7)–C(8)	1.419(3)	C(8)–C(9)	1.364(3)	C(7)–C(8)–C(9)	126.7(2)	C(7)–C(8)–C(16)	123.0(2)
C(8)–C(16)	1.503(3)	C(9)–C(10)	1.458(3)	C(9)–C(8)–C(16)	110.3(2)	C(8)–C(9)–C(10)	109.2(2)
C(10)–C(15)	1.404(3)	C(10)–C(11)	1.385(3)	C(8)–C(16)–C(15)	103.0(2)	C(9)–C(10)–C(15)	108.3(2)
C(14)–C(15)	1.379(3)	C(15)–C(16)	1.496(3)	C(10)–C(15)–C(16)	109.2(2)	C(6)–C(1)–C(2)	128.4(2)
2							
C(10)–C(11)	1.459(5)	C(11)–C(12)	1.402(4)	C(6)–C(10)–C(11)	128.1(3)	C(9)–C(10)–C(11)	125.7(3)
C(14)–C(17)	1.438(6)	C(17)–C(18)	1.181(5)	C(13)–C(14)–C(17)	121.8(3)	C(15)–C(14)–C(17)	120.3(4)
C(18)–C(19)	1.416(6)	C(19)–C(20)	1.355(5)	C(14)–C(17)–C(18)	175.4(4)	C(17)–C(18)–C(19)	177.7(4)
C(19)–C(27)	1.480(5)	C(20)–C(21)	1.443(5)	C(18)–C(19)–C(20)	126.6(4)	C(18)–C(19)–C(27)	123.7(3)
C(21)–C(26)	1.398(4)	C(26)–C(27)	1.489(5)	C(19)–C(27)–C(26)	104.1(3)	C(20)–C(19)–C(27)	109.7(3)
4							
C(5)–C(6)	1.430(6)	C(6)–C(7)	1.201(6)	C(5)–C(6)–C(7)	176.9(6)	C(6)–C(7)–C(8)	175.1(6)
C(7)–C(8)	1.425(6)	C(11)–C(14)	1.478(6)	C(7)–C(8)–C(9)	121.5(4)	C(11)–C(14)–C(15)	124.7(4)
C(14)–C(15)	1.410(6)	C(14)–C(22)	1.426(6)	C(11)–C(14)–C(22)	123.9(4)	C(14)–C(22)–C(21)	105.5(4)
C(15)–C(16)	1.494(6)	C(16)–C(21)	1.408(6)	C(14)–C(15)–C(16)	106.6(4)	C(32)–C(33)–C(34)	175.9(6)
C(21)–C(22)	1.486(6)	C(41)–C(42)	1.426(6)	C(33)–C(34)–C(35)	177.3(6)	C(41)–C(42)–C(43)	106.6(4)
C(41)–C(49)	1.436(6)	C(48)–C(49)	1.473(6)	C(41)–C(49)–C(48)	106.8(4)	C(42)–C(41)–C(49)	109.7(4)

demonstrating conjugated double bond and non-conjugated single bonds in the five-membered ring of indenyl. The bond angles [C(17)–C(18)–C(19), 177.7(4)°; C(14)–C(17)–C(18), 175.4(4)°], and torsion angle [C(10)–C(11)–C(14)–C(17), 4.22°] demonstrate that the carbon chain C(10)C(11)C(14)C(17)C(18)C(19) is nearly linear. The dihedral angle between planes [C(1)C(2)C(3)C(4)C(5)] and [C(6)C(7)C(8)C(9)C(10)] is 1.25°, showing that two Cp planes of the ferrocenyl group are nearly parallel. The dihedral angle between Cp plane [C(6)C(7)C(8)C(9)C(10)] and phenyl ring plane [C(11)C(12)C(13)C(14)C(15)C(16)] is 7.68°, slightly deviated from parallel. The dihedral angle between the phenyl ring [C(11)C(12)C(13)C(14)C(15)C(16)] and indenyl planes [C(19)C(20)C(21)C(22)C(23)C(24)C(25)C(26)C(27)] is 13.39°. Hence, **2** is also a partially conjugated system.

Compounds **2** and **4** are a pair of isomeric compounds, where ferrocenyl and indenyl units are connected *via* the phenyl-ethynyl units with different sequence (figures 2 and 3). Crystals of **4** are twin molecules as repeating unit in the cell (figure 4), resulting from intermolecular interactions. The C–H of one molecule and π bond of another molecule form a C–H $\cdots\pi$ hydrogen bond; this also appears in other molecules [22]. In C–H $\cdots\pi$ system of **4**, hydrogen bond lengths of H(13)–C(46), H(22B)–C(41), H(20)–C(36), and H(20)–C(37) are 2.863, 2.885, 2.835, and 2.862 Å, respectively (figure 4).

For **4**, the C(6)–C(7) and C(33)–C(34) bond lengths are 1.201(6) and 1.197(6) Å, respectively, longer than that in **2**. The C(5)–C(6), C(7)–C(8), C(34)–C(35), and C(32)–C(33) bond lengths are 1.430(6), 1.425(6), 1.425(6), and 1.422(6) Å, similar to those in **1** and **2**. Bond lengths of C(22)–C(14), C(14)–C(15), C(16)–C(15), C(41)–C(42), and C(41)–C(49) are 1.426(6), 1.410(5), 1.494(6), 1.426(6), and 1.436(6) Å, respectively, which are longer than in **1** and **2** due to the intermolecular interactions of C–H of indenyl to the π system of another molecule (figure 4). The torsions angles of [C(5)–C(6)–C(7)–C(8), 4.39°; C(14)–C(11)–C(8)–C(7), 7.25°] demonstrate that the carbon chain C(14)C(11)C(8)C(7)C(6)C(5) is also nearly linear.

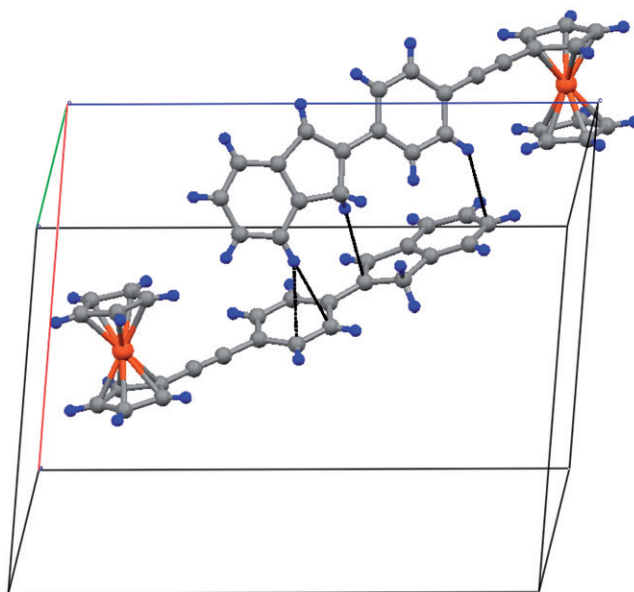


Figure 4. The C–H··· π hydrogen bond in **4**.

In figure 3, two molecules are designated 4-1 and 4-2. The dihedral angles [$1.64(0.29)^\circ$ for 4-1 and $2.22(0.34)^\circ$ for 4-2] show that the C5 and C6 rings of two indenyls are nearly on one plane. The dihedral angles [$5.18(0.27)^\circ$ for 4-1; $8.97(0.30)^\circ$ for 4-2] between the C5 ring plane of the indenyl and the phenyl ring plane demonstrate that the indenyl and phenyl rings slightly deviate from parallel. The dihedral angle between the [C(1)C(2)C(3)C(4)C(5)] plane of ferrocenyl and [C(8)C(9)C(10)C(11)C(12)C(13)] plane of phenyl in 4-1 is $66.04(0.15)^\circ$, larger than the dihedral angle [$14.22(0.30)^\circ$] between the [C(28)C(29)C(30)C(31)C(32)] and the [C(35)C(36)C(37)C(38)C(39)C(40)] planes in 4-2. The planes of phenyl, indenyl, and ferrocenyl groups lean to perpendicularity in 4-1 and phenyl, indenyl, and ferrocenyl groups tend to parallelism in 4-2. The changes of dihedral angles in **4** further show C–H··· π hydrogen bonds between 4-1 and 4-2 (figure 4), which are important in controlling crystal spatial conformation of **4**.

3.3. Cyclic voltammetric study of **1**, **2**, **3**, and **4**

The redox potential differences of **1–4** were investigated by cyclic voltammetry (Supplementary material). For **1** with ferrocenyl unit connected to indenyl by an acetylene bridge directly, the half-wave potential, $E_{1/2}(\mathbf{1})$, is 0.130 V. With a phenyl introduced between ferrocenyl and acetylenyl, $E_{1/2}(\mathbf{2})$ is positively shifted to 0.190 V. The positive shift can be ascribed to the effect of electron delocalization with enlargement of the conjugated system; more electrons of the ferrocenyl unit were transferred to the whole system with the enlargement of the conjugated system. This could also be illustrated through the fact that on increasing half-wave potential of **3** with an acetylenyl inserted into phenyl and ferrocenyl, the conjugated system was

further enlarged and $E_{1/2}(\mathbf{3})$ increased to 0.216 V. The half-wave potential, $E_{1/2}(\mathbf{4})$, was 0.220 V, notwithstanding the conjugated system of $\mathbf{4}$ being similar to that of $\mathbf{2}$. Two molecules interact *via* C–H $\cdots\pi$ hydrogen bond to swell the conjugated system of $\mathbf{4}$.

In order to understand the potential difference of ferrocenes in $\mathbf{1}$ – $\mathbf{4}$, we further calculated the extended Hückel charge of Fe(II) in the HOMO orbitals of $\mathbf{1}$, $\mathbf{2}$, and $\mathbf{4}$ (Supplementary material) *via* the single crystal structural data. The extended Hückel charge of Fe(II) in the HOMO of $\mathbf{1}$, $\mathbf{2}$, and $\mathbf{4}$ were -1.84218 , -1.80177 , and -1.77663 , respectively, which indicated that the charge density of Fe(II) in $\mathbf{4}$ was the lowest and the charge density of Fe(II) in $\mathbf{1}$ was the highest, consistent with the half-wave potential of $\mathbf{1}$ the lowest and that of $\mathbf{4}$ the highest.

4. Conclusion

Four ferrocenyl indenyl derivatives $\text{C}_9\text{H}_7\text{C}\equiv\text{C}\text{Fc}$ ($\mathbf{1}$), $\text{C}_9\text{H}_7\text{C}\equiv\text{C}\text{C}_6\text{H}_5\text{Fc}$ ($\mathbf{2}$), $\text{C}_9\text{H}_7\text{C}\equiv\text{C}\text{C}_6\text{H}_5\text{C}\equiv\text{C}\text{Fc}$ ($\mathbf{3}$), and $\text{C}_9\text{H}_7\text{C}_6\text{H}_5\text{C}\equiv\text{C}\text{Fc}$ ($\mathbf{4}$), were synthesized by cross-coupling reactions. The molecular structures of $\mathbf{1}$, $\mathbf{2}$, and $\mathbf{4}$ were characterized by X-ray single crystal diffraction technique. Cyclic voltammetry and calculations showed that the redox potential of the ferrocenyl unit increased with enlargement of the conjugated system of the ferrocenyl indenyl derivatives. Usually, positive shift of the redox potentials of ferrocenyl units is attributed to the effect of electron-withdrawing groups [32–34], but in the present system, enlargement of the conjugated system exhibited similar effect.

Supplementary material

CCDC 701552, 701553, and 701554 contain the supplementary crystallographic data for $\mathbf{1}$, $\mathbf{2}$, and $\mathbf{4}$, respectively. These data can be obtained free of charge *via* <http://www.ccdc.cam.ac.uk/conts/retrieving.html>, or from the Cambridge Crystallographic Data Centre, 12 Union Road, Cambridge CB2 1EZ, UK; Fax: (+44) 1223-336-033; or E-mail: deposit@ccdc.cam.ac.uk.

Acknowledgments

We thank the Program for New Century Excellent Talents in University (NCET-08-858), the Natural Science Foundation of the Inner Mongolia (20080404MS020) and Specialized Research Fund of Inner Mongolia University of Technology (ZD200704).

References

- [1] M. Thimmaiah, R.L. Luck, S.Y. Fang. *J. Organomet. Chem.*, **692**, 1956 (2007).
- [2] O.J. Curnow, G.M. Fern. *J. Organomet. Chem.*, **690**, 3018 (2005).
- [3] D. Zargarian. *Coord. Chem. Rev.*, **233**, 157 (2002).
- [4] M.J. Calhorda, V. Felix, L.F. Veiros. *Coord. Chem. Rev.*, **230**, 49 (2002).
- [5] V. Cadierno, J. Diez, M.P. Gamasa, J. Gimeno, E. Lastra. *Coord. Chem. Rev.*, **193**, 147 (1999).
- [6] P. Witte, T.K. Lal, R.M. Waymouth. *Organometallics*, **18**, 4147 (1999).
- [7] M.E. Rerek, L.N. Ji, F. Basolo. *J. Chem. Soc., Chem. Commun.*, 1208 (1983).
- [8] A. Ceccon, S. Santi, L. Orian, A. Bisello. *Coord. Chem. Rev.*, **248**, 683 (2004).
- [9] B.Y. Lee, Y.K. Chung. *J. Am. Chem. Soc.*, **116**, 8793 (1994).
- [10] S. Santi, L. Orian, C. Durante, A. Bisello, F. Benetollo, L. Crociani, P. Ganis, A. Ceccon. *Chem. Eur. J.*, **13**, 1955 (2007).
- [11] S. Santi, L. Orian, A. Donoli, C. Durante, A. Bisello, P. Ganis, A. Ceccon. *Organometallics*, **26**, 5867 (2007).
- [12] S. Santi, F. Benetollo, A. Ceccon, L. Crociani, A. Gambaro, P. Ganis, M. Tiso, A. Venzo. *Inorg. Chim. Acta*, **344**, 221 (2003).
- [13] S. Santi, A. Ceccon, L. Crociani, A. Gambaro, P. Ganis, M. Tiso, A. Venzo, A. Bacchi. *Organometallics*, **21**, 565 (2002).
- [14] J. Lin, B.Q. Wang, S.S. Xu, H.B. Song. *J. Organomet. Chem.*, **691**, 2528 (2006).
- [15] P.E. Gaede. *J. Organomet. Chem.*, **616**, 29 (2000).
- [16] H. Plenio. *Organometallics*, **11**, 1856 (1992).
- [17] S. Santi, A. Ceccon, L. Crociani, A. Gambaro, P. Ganis, M. Tiso, A. Venzo, A. Bacchi. *Organometallics*, **21**, 565 (2002).
- [18] V.S. Sridevi, W.K. Leong. *J. Organomet. Chem.*, **692**, 4909 (2007).
- [19] S. Santi, A. Ceccon, A. Bisello, C. Durante, P. Ganis, L. Orian. *Organometallics*, **24**, 4691 (2005).
- [20] V. Cadierno, M.P. Gamasa, J. Gimeno. *Organometallics*, **18**, 2821 (1999).
- [21] S.G. Lee, S.S. Lee, Y.K. Chung. *Inorg. Chim. Acta*, **286**, 215 (1999).
- [22] M. Nishio. *Cryst. Eng. Comm.*, **6**, 130 (2004).
- [23] T.M. Keller, S.B. Qadri. *Chem. Mater.*, **16**, 1091 (2004).
- [24] C.R. Simionescu, T. Lixandru, I. Mazilu, L. Tataru. *J. Organomet. Chem.*, **113**, 23 (1976).
- [25] Q.L. Suo, Y.Q. Ma, Y.B. Wang, L.M. Han, Y.G. Bai, L.H. Weng. *J. Coord. Chem.*, **61**, 1234 (2008).
- [26] B.R. Waldbaum, R.C. Kerber. *Inorg. Chim. Acta*, **291**, 109 (1999).
- [27] K. Takahashi, Y. Kurayama, K. Sonogashira, N. Hagihara. *Synthesis*, **8**, 627 (1980).
- [28] G.M. Sheldrick. *Acta Cryst. A*, **46**, 467 (1990).
- [29] G.M. Sheldrick. *SADABS, Siemens Area Detector Absorption, Correction Software*, University of Göttingen, Germany (1997).
- [30] Bruker. *SMART and SAINT, Area Detector Control and Integration Software*. Bruker Analytical X-ray Instruments Inc., Madison, Wisconsin, USA (1998).
- [31] Bruker. *SHELXTL*, Bruker Analytical X-ray Instruments Inc., Madison, Wisconsin, USA (1997).
- [32] L.M. Han, Y.Q. Hu, Q.L. Suo, M.H. Luo, L.H. Weng. *J. Coord. Chem.*, **63**, 600 (2010).
- [33] R.J. Xie, L.M. Han, Q.L. Suo, H.L. Hong, M.H. Luo. *J. Coord. Chem.*, **63**, 1700 (2010).
- [34] C.J. Qiao, J. Li, Y. Xu, S.Y. Guo, X. Qi, Y.T. Fan. *J. Coord. Chem.*, **62**, 3268 (2009).